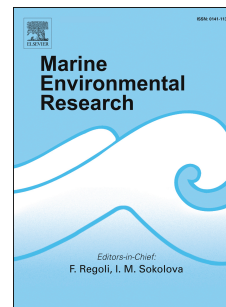


Journal Pre-proof

Oxidative stress, lysosomal damage and dysfunctional autophagy in molluscan hepatopancreas (digestive gland) induced by chemical contaminants

J.P. Shaw, M.N. Moore, J.W. Readman, Z. Mou, W.J. Langston, D.M. Lowe, P.E. Frickers, L. Al-Moosawi, C. Pascoe, A. Beesley



PII: S0141-1136(19)30470-2

DOI: <https://doi.org/10.1016/j.marenvres.2019.104825>

Reference: MERE 104825

To appear in: *Marine Environmental Research*

Received Date: 23 July 2019

Revised Date: 10 October 2019

Accepted Date: 13 October 2019

Please cite this article as: Shaw, J.P., Moore, M.N., Readman, J.W., Mou, Z., Langston, W.J., Lowe, D.M., Frickers, P.E., Al-Moosawi, L., Pascoe, C., Beesley, A., Oxidative stress, lysosomal damage and dysfunctional autophagy in molluscan hepatopancreas (digestive gland) induced by chemical contaminants, *Marine Environmental Research* (2019), doi: <https://doi.org/10.1016/j.marenvres.2019.104825>.

This is a PDF file of an article that has undergone enhancements after acceptance, such as the addition of a cover page and metadata, and formatting for readability, but it is not yet the definitive version of record. This version will undergo additional copyediting, typesetting and review before it is published in its final form, but we are providing this version to give early visibility of the article. Please note that, during the production process, errors may be discovered which could affect the content, and all legal disclaimers that apply to the journal pertain.

© 2019 Published by Elsevier Ltd.

Oxidative stress, lysosomal damage and dysfunctional autophagy in molluscan hepatopancreas (digestive gland) induced by chemical contaminants

J.P. Shaw¹, M.N. Moore^{1,2,3*}, J.W. Readman^{1,3}, Z. Mou¹, W.J. Langston⁴, D.M. Lowe¹, P.E. Frickers¹, L. Al-Moosawi¹, C. Pascoe¹ & A. Beesley¹

¹ Plymouth Marine Laboratory, Prospect Place, The Hoe, Plymouth, Devon, PL1 3DH, UK

² European Centre for Environment & Human Health (ECEHH), University of Exeter Medical School, Knowledge Spa, Royal Cornwall Hospital, Truro, TR1 3HD, UK

³ School of Biological & Marine Sciences, University of Plymouth, Drake Circus, Plymouth, PL4 8AA, UK

⁴ Marine Biological Association UK, Citadel Hill, Plymouth, Devon, PL1 2PB, UK

* Corresponding author: Prof. M N Moore, Plymouth Marine Laboratory, Prospect Place, West Hoe, Plymouth, Devon, PL1 3DH, UK; Tel: +44(0)1579 389006; Fax +44 (0)1752 633101; E-mail: mnm@pml.ac.uk

Two line capsule of paper:

Oxidative stress was induced by a range of contaminants in two marine molluscs resulting in dysfunctional lysosomal autophagy in digestive gland cells.

Keywords: lysosomal membrane stability; dysfunctional autophagy; lipofuscinosis; lipidosis; oxidative stress; molluscs; hepatopancreas/digestive gland; chemical pollutants.

Abstract

Autophagy is a highly conserved evolutionary survival or defence process that enables cells and organisms to survive periods of environmental stress by breaking down cellular organelles and macromolecules in autolysosomes to provide a supply of nutrients for cell maintenance. However, autophagy is also a part of normal cellular physiology that facilitates the turnover of cellular constituents under normal conditions: it can be readily augmented by mild environmental stress; but becomes dysfunctional with severe oxidative stress leading to cellular pathology. The molluscan hepatopancreas or digestive gland provides a versatile and environmentally relevant model to investigate lysosomal autophagy and stress-induced dysfunctional autophagy. This latter process has been implicated in many animal and human disease conditions, including degenerative and neurodegenerative diseases, as well as obesity related conditions. Many environmental pollutants have also been found to induce dysfunctional autophagy in molluscan hepatopancreatic digestive cells, and in this study, the marine blue mussel *Mytilus galloprovincialis* was exposed for 7 days to: 0.1 μM , 1 μM and 10 μM concentrations of fluoranthene and phenanthrene (PAHs); chlorpyrifos and malathion (organophosphorus compounds); atrazine (triazine herbicide); copper (transition metal) and dodecylbenzene sulphonic acid (LAS, surfactant). The marine snail or periwinkle, *Littorina littorea*, was also exposed to phenanthrene, chlorpyrifos and copper. Indices of oxidative stress, cell injury and dysfunctional autophagy were measured (i.e., lysosomal membrane stability, protein carbonyls, lipofuscin, and lysosomal accumulation of lipid or lipidosis). Evidence of oxidative stress, based on the elevation of lipofuscin and protein carbonyls, was found for all compounds tested; with chlorpyrifos being the most toxic to both species. Dysfunctional autophagy was induced by all of the compounds tested in both species, except for atrazine in mussels. This failure of normal autophagy was consistently associated with oxidative stress. Autophagic dysfunction is an important emerging feature in the aetiology of many disease conditions in animals and humans; and an explanatory conceptual mechanistic model has been developed for dysregulation of autophagy in response to oxidative stress.

Introduction

Autophagy is a highly conserved evolutionary survival or defence process that enables cells and organisms to survive periods of environmental stress by breaking down cellular organelles and macromolecules in autolysosomes to provide a supply of nutrients for cell maintenance (Cuervo, 2004, 2008; Klionsky et al., 2016). However, autophagy is also a part of normal cellular physiology that facilitates the turnover of cellular constituents under normal conditions: it can be readily augmented by mild environmental stress; but becomes dysfunctional with severe stress, such as oxidative stress, leading to cellular injury, with consequent tissue atrophy and organ pathology and reduction in physiological scope for growth (Boya, 2012; Cuervo, 2004, 2008; Lowe, 1988; Moore, 1982, 1988; Moore et al., 2006a, 2007a, b, 2015; Numan et al., 2015; Sforzini et al., 2018; Shaw et al., 2011). The molluscan hepatopancreas or digestive gland is a liver analogue that provides a versatile and environmentally relevant model to investigate lysosomal autophagy and stress induced dysfunctional autophagy (Lowe et al., 2006; Moore et al., 2006a, b, 2007b; Sforzini et al., 2018; Shaw et al., 2011). This latter process has been implicated in many animal and human disease conditions, including fibromyalgia, degenerative and neurodegenerative diseases, as well as obesity related conditions (Chen et al., 2012; Colacurcio et al 2018; Jiang & Mizushima, 2014; Namkoong et al., 2018; Nixon, 2013; Numan et al., 2015; Oezel et al., 2016).

Molluscan digestive cells have a highly developed lysosomal-vacuolar system that is essential for the digestion of endocytosed food particles by the process of intracellular digestion: the major component of digestion in mussels and periwinkles (Moore et al., 2006a; Moore, 1988). In addition to this heterophagic lysosomal digestion, digestive cells also have a highly developed capacity for lysosomally mediated autophagic digestion of cellular constituents including organelles and macromolecules (Koukouzika et al., 2009; Lowe, 1988; Moore et al., 2006a, 2007a, b; Sforzini et al., 2018). Effective performance of the autophagic processes is essential for the normal recycling of damaged and redundant proteins and organelles, as well as mobilisation of stored reserves for gametogenesis (Bayne et al., 1978; Lowe et al., 1982). Autophagy has a protective role in physiological responses to low-level environmental stress: however, more severe stress results in functional perturbation of autophagy leading to the pathological reactions described as dysfunctional autophagy (Boya, 2012; Cuervo, 2004; Dimitriadis

et al., 2004; Domouhtsidou et al. 2001; Moore, 2008; Moore et al., 2006b, 2008; Numan et al., 2015; Sforzini et al., 2018; Shaw et al., 2011).

Many environmental pollutant chemicals can induce oxidative stress that, in turn, can contribute to autophagic responses (Moore et al., 2006a, 2007b). If the oxidative stress becomes severe then the initial protective autophagic response can lead to a pathological dysfunctional autophagic reaction (Moore, 2008, 2010). Industrial and domestic incomplete combustion processes and oil spills, as well as vehicle emissions and road/tyre dust contribute to the influx of polycyclic aromatic hydrocarbons in air pollution and into the aquatic environment (Cajaraville et al., 1995; Numan et al., 2015; Shaw et al., 2011). Pest control and agricultural use are major contributors to the release of herbicides and pesticides into the aquatic environment. Environmental contaminants tested in the current study of oxidative stress, lysosomal damage and dysfunctional lysosomal autophagy include polycyclic aromatic hydrocarbons (phenanthrene & fluoranthene), pesticides (malathion & chlorpyrifos) a herbicide (atrazine), a surfactant (sodium dodecylbenzene sulphonate - LAS) and the transition metal copper (Moore et al., 2018; Readman et al., 2002). Copper, a known inducer of oxidative stress, has been, and is still, a global priority pollutant of fresh and marine waters (Hamed et al. 2006; Langston et al., 1999). These chemicals have been chosen on the basis of their well-documented toxicity and their continued presence in the environment in various parts of the world (Cassee et al., 1998; LeBlanc & Olmstead, 2004).

The aim of this investigation was to test for the induction of dysfunctional autophagy in molluscan hepatopancreatic digestive cells, associated with oxidative stress, by deploying biomarkers of cellular health in the marine blue mussel *Mytilus galloprovincialis* treated with fluoranthene and phenanthrene (PAHs); chlorpyrifos and malathion (OP - organophosphorus compounds); atrazine (triazine herbicide); copper (transition metal) and LAS (surfactant), at concentrations of 0.1 μ M, 1 μ M and 10 μ M, for 7 days. In addition, marine snails or periwinkles (*Littorina littorea*) were also treated with chlorpyrifos, phenanthrene and copper at the same concentrations and for the same time period as the mussels. Animal health was assessed by measuring indices of oxidative damage and autophagy (protein carbonyls and lysosomal lipofuscin - lipofuscinosis), cellular health (lysosomal membrane damage) and fatty change (equivalent to steatosis in mammalian liver); with a pathological dysfunctional autophagic

accumulation of triglyceride (lipidosis) in abnormally enlarged autolysosomes (Domouhtsidou et al. 2001; Lowe, 1988; Moore, 1988; Moore et al., 2006a, 2007b). Data for lysosomal and oxidative stress biomarkers was synthesised using multivariate analysis, with the first principal component being used as an integrated index of “health status” (Allen & Moore, 2004; Moore et al., 2006a; Sforzini et al., 2018).

Materials & Methods

Chemicals

Most chemicals were obtained from Sigma-Aldrich, unless stated otherwise. Anthracene and phenanthrene were > 99% pure; LAS (dodecylbenzene sulphonate) was Pharmaceutical Secondary Standard - Certified Reference Material; pesticides and herbicides were analytical standard grade; DMSO (> 99.9%); and neutral red powder (N4638) was graded as suitable for cell culture. Other reagents used were of ANALAR grade. Cytochemical substrates for lysosomal hydrolases, naphthol-AS-BI-N-acetyl- β -glucosaminide and naphthol-AS-BI- β -glucuronide, were obtained from Sigma-Aldrich. The diazonium coupler fast red-violet LB was obtained from Difco Laboratories. The anti-DNPH (dinitrophenyl) primary antibody (A6435), Nanogold secondary antibody (A-24926) and the silver enhancement kit (L24919) were purchased from Molecular Probes, UK.

Animal Husbandry and Experimental Treatments

Mussels *Mytilus galloprovincialis* (4.8 – 5.2 cm) were collected from Trebarwith Strand, North Cornwall, U.K. (avoiding the spawning period); and periwinkles (littorinids) *Littorina littorea* (2 - 2.5 cm) were collected from Port Quin, North Cornwall, U.K. The animals were placed in 34 psu, $15 \pm 1^\circ\text{C}$, $1 \mu\text{m}$ filtered sea water (aerated) to acclimate for one week. Sea water was replaced daily. Mussels were fed 30 mg/animal/day of dried kelp continuously via a peristaltic pump throughout the exposures and periwinkles were fed green sea lettuce *Ulva* (collected from Port Quin) *ab libitum*. The animals were divided into five treatments: control (C), solvent or vehicle control (VC; 0.02% DMSO), and 0.1 μM , 1 μM and 10 μM initial chemical concentrations, which were renewed on a daily basis. Mussels were treated in 10L polypropylene tanks (10 animals/tank and natural daylight regime) with atrazine, chlorpyrifos, copper, fluoranthene, dodecylbenzene sulphonic acid (a linear alkylbenzene sulphonate, LAS), malathion and phenanthrene. Periwinkles were exposed as with the mussels to chlorpyrifos, copper and

phenanthrene. Neither Cu nor malathion required the use of a solvent (DMSO). Animals were dosed with the contaminant each day for 7 days and sampled on day 0 and day 7. Digestive glands were carefully removed, plunged into liquid nitrogen and stored at -40°C.

Chemical Analyses – Water and Digestive Gland

Fluoranthene, phenanthrene, chlorpyrifos, malathion and atrazine analyses

Half an hour after the contaminant was added to the exposure vessels, 250 ml water samples were removed, taking care to avoid the putative surface microlayer, and placed in acid washed, hexane rinsed, stoppered glass vessels. 50 ml of dichloromethane (DCM) was added to stabilize the samples before being kept at 4°C until analysis (DCM was omitted for Cu samples). The samples were analysed for organic contaminants essentially as described by Kelly et al. (2000). The clean-up was derived from Readman et al. (2002), and was rigorously tested for performance/recoveries using spiked standards.

Water samples (including the DCM) were spiked with an internal deuterated standard, mixed and then transferred directly to a glass separating flask fitted with a PTFE tap. The phases were shaken vigorously for 2 minutes and allowed to settle for a further 2 min before the solvent phase was run off into round bottomed flasks. This extraction procedure was repeated twice with additional DCM. The combined DCM fraction was dried using a small amount of anhydrous sodium sulphate (Na_2SO_4). To remove the Na_2SO_4 , the extracts were transferred to a second series of round bottom flasks with rinsings from the original flasks. The extracts were concentrated down to ~ 2 ml using a BUCHI rotary evaporator before being transferred to the final analysis vials and blown down to 1 ml. Analysis was performed using gas chromatography mass spectrometry. 1 µl of sample was injected into a 30 m x 0.250 DB-5MS column with helium used as the carrier gas. The injector was set on splitless, with a temperature of 250°C. The oven had an initial temperature of 40°C which was held for 2 mins before being ramped at 6°C per min to reach a final temperature of 300°C.

Digestive glands and remainder tissues were stored at -80°C prior to analysis (Law et al., 1999). The samples were allowed to defrost at room temperature. A sub-portion was freeze dried to obtain moisture content. The mussel tissues were weighed into round

bottom flasks, spiked with a deuterated internal standard and digested by adding 20 g of potassium hydroxide pellets and 100 ml of methanol (saponification). The samples were refluxed for 4 hours and filtered through glass fibre filters. The filtrate was placed into separating flasks with 50 ml *n*-pentane and shaken for 2 min and allowed to settle and separate for a further 2 min after which the phases were separated by running off the lower layer and collecting the upper *n*-pentane layer. This extraction procedure was carried out a second time and the *n*-pentane layers combined and dried over Na₂SO₄. The samples were reduced to ~5ml by rotary evaporation. Due to the release of lipids and co-extractives a clean up using alumina and silica was required.

To ensure the quality of the analytical results, reagent blanks and recoveries were run with each batch. Good quantitative data was achieved using relevant deuterated internal standards. Instrument calibration and instrument response factors were run and calculated for each batch of analyses.

LAS analysis in water

LAS was determined by fluorimetry, using a Perkin Elmer LS-50B fluorometer and FLWinlab program. New standards were prepared on a daily basis to prevent standard degradation. The standard range was 0 – 2.5 mg/L and quenching occurred around 3 mg/L. No sample preparations were necessary and both standards and samples were analysed using a quartz cuvette under the following conditions: excitation wavelength – 231 nm; emission wavelength – 301 nm; excitation slit width -10 nm; emission slit width – 10 nm; emission filter – 350 nm cut off.

Chlorpyrifos, malathion and LAS were not measured in tissue because they are comparatively polar, are difficult to extract and isolate, and tend not to bioaccumulate.

Cu determination

Copper was determined using a combination of flame and graphite furnace atomic absorption spectrophotometry, depending on concentration. Analysis of tissues was performed on freeze-dried samples following microwave digestion in high purity (Aristar) nitric acid. (Langston et al. 1999).

Cytochemical Determinations for Lysosomal Stability, Lipofuscin and Lysosomal Neutral Lipids

The following assays were all performed on 10 μm frozen sections of mussel and periwinkle digestive gland. Lipofuscin was determined *via* the Schmorl assay as described by Moore (1988). Lysosomal membrane stability was measured by determining the latency period for N-acetyl- β -hexosaminidase activity (mussels), and β -glucuronidase (periwinkles) (Moore, 1988; Moore et al., 2008; Sforzini et al., 2018). Lysosomal accumulation of neutral lipids (triglycerides) was determined using the Oil Red O method (Moore et al., 2008). Lipofuscin and lysosomal neutral lipid were assessed using series of micrographs based on increasing relative absorbance of their respective cytochemical reaction product (Moore 1988; Moore et al., 2006a, 2007b, 2008).

Immunocytochemical Determination for Protein Carbonyls

Protein carbonyls were determined immunocytochemically in 10 μm frozen sections of digestive gland method using a modified 2,4-dinitrophenylhydrazine detection method (Alamdari et al., 2005; Frank et al., 2005; Smith et al., 1998; Shaw et al., 2011). Following sectioning, the sections were mounted on slides and air dried at room temperature for 1 hour. Subsequently, the sections were fixed in Baker's calcium formal fixative solution (10% formaldehyde, 2.5% sodium chloride, 1% calcium chloride) for 5 minutes at 4°C. The slides were rinsed in distilled water before being incubated in 2,4-dinitrophenylhydrazine (10 mM DNPH in 6M guanidine hydrochloride, 0.5 M potassium phosphate buffer, pH 2.5) solution for 45 min at room temperature in a humidity box in the dark (Alamdari et al., 2005; Frank et al., 2005; Smith et al., 1998). Following this, the slides were rinsed in distilled water followed by PBS for 10 minutes, and a blocking solution was applied (non-fat dried milk 1:10 in PBS) for 10 minutes. The slides were placed in anti-DNPH (1:100 in PBS) overnight at 4°C. The slides were then rinsed in PBS before being incubated in nano-gold secondary antibody overnight at 4°C. Following this, the slides were washed in sodium citrate buffer (3 M sodium chloride, 300 mM sodium citrate, pH 7) before silver enhancement. Protein carbonyls were assessed by construction of a series of micrographs based on increasing protein carbonyl immunocytochemical reaction product density (Moore 1988; Moore et al., 2008; Shaw et al., 2011).

Univariate Statistical Analysis

The non-parametric Mann-Whitney *U*-test was used to compare the data from treated animals with those of the controls (Sforzini et al., 2018).

Multivariate Analysis

Biomarker data for mussels and periwinkles exposed to the seven test chemicals were analysed using non-parametric multivariate analysis software, PRIMER v 6 (PRIMER-E - University of Auckland, New Zealand; Clarke, 1999; Clarke & Warwick, 2001; Moore et al., 2006a). All data were log transformed [$\log_n(1 + x)$] and standardised to the same scale. Correlations between biomarkers were tested using a scatter plot matrix (PRIMER v 6, Draftsman Plot). Principal component analysis (PCA) and hierarchical cluster analysis, derived from Euclidean distance similarity matrices were used to visualise dissimilarities between sample groups. The results were further tested for significance using analysis of similarity (PRIMER v6 - ANOSIM), which is an approximate analogue of the univariate ANOVA and reflects on differences between treatment groups in contrast to differences among replicates within samples (the *R* statistic). Under the null hypothesis H_0 ("no difference between samples"), $R = 0$ and this was tested by a non-parametric permutations approach; there should be little or no effect on the average *R* value if the labels identifying which replicates belong to which samples are randomly rearranged.

Finally, in order to map integrated biomarker data onto "health status space", measured primarily as the first principal component - PC1 for the biomarker data, the individual biomarkers were correlated with PC1 from the integrated evaluation (Allen and Moore, 2004; Moore et al., 2006a; Sforzini et al., 2015, 2017, 2018).

Results

Chemistry (see Table 1)

No nominal water values matched the dose concentrations. This probably resulted from several factors. Water samples were not taken for half an hour after sampling, to allow dispersal, however during this period the contaminants may have sorbed onto the exposure tanks surfaces, suspended particulate matter or the animals themselves. Alternatively, they may have been ingested, in particular by the filter feeding mussels.

Tissue concentrations of the xenobiotics measured indicated that the two PAHs were accumulated in mussel digestive gland (Table 1). Phenanthrene accumulated in the periwinkle digestive gland; but to a lesser extent than in the mussels (Table 1). Copper accumulated in both species, and the concentrations in the periwinkle digestive gland were greater than in the mussels (Table 1).

Biomarkers (see Table 2: summary of results; Figures 1-5)

Lipofuscin

Lipofuscin in mussels was increased significantly ($p \leq 0.05$) at all exposure concentrations for both phenanthrene and fluoranthene (Fig. 1). Lipofuscin was also elevated at 0.1 μM and 10 μM for malathion (Fig. 1). Lipofuscin was only significantly higher within the 10 μM exposure mussels for LAS, copper and chlorpyrifos, while there were no significant changes following atrazine exposure (Fig. 1).

Lipofuscin in littorinid snails was significantly ($p \leq 0.05$) elevated in all exposure concentrations for phenanthrene (Fig. 5). Lipofuscin was significantly higher in the 1 μM and 10 μM animals exposed to chlorpyrifos, while the 10 μM concentration of copper induced a significant increase (Fig. 5).

Lysosomal membrane stability (based on latency of N-acetyl- β -hexosaminidase for mussels & β -glucuronidase for littorinids)

Mussel lysosomal stability was significantly decreased ($p \leq 0.05$) in all concentrations for chlorpyrifos (Fig. 2), and in the 1 μM and 10 μM concentrations for atrazine (Fig. 2), fluoranthene, phenanthrene (Fig. 2) and malathion (Fig. 2). Lysosomal stability was only seen to significantly decrease in 10 μM copper and LAS treatments (Fig. 2).

Periwinkle lysosomal stability significantly decreased at all concentrations for chlorpyrifos, at 1 μM and 10 μM for phenanthrene, and only at the 10 μM copper concentration (Fig. 5).

Fatty change & autolysosomal lipids (triglycerides)

Mussel neutral lipids (triglycerides), within swollen autolysosomes (i.e., increase in lysosomal/cytoplasmic volume ratio – L/C vol), were increased significantly ($p \leq 0.05$) in all chlorpyrifos exposure treatments (Fig. 3). Lipids were also significantly elevated in the

10 μM LAS, 1 μM fluoranthene and 0.1 μM copper treatments (Fig. 3). However, neutral lipids were significantly decreased in the 1 μM and 10 μM malathion exposures (Fig. 3); and there were no differences in lipids in mussels exposed to atrazine (Fig. 3).

Periwinkle neutral lipids, again within swollen autolysosomes, were significantly elevated ($p \leq 0.05$) in all exposure treatments for chlorpyrifos and copper; and in the 1 μM and 10 μM phenanthrene treatments Fig. 5).

Protein carbonyls

Mussel protein carbonyls were significantly ($p \leq 0.05$) elevated in the 1 μM and 10 μM atrazine, copper, fluoranthene and LAS exposure treatments and in the 10 μM chlorpyrifos, malathion and phenanthrene treatments (Fig. 4).

Periwinkle protein carbonyls were significantly ($p \leq 0.05$) increased in the 1 μM and 10 μM chlorpyrifos and phenanthrene treatments; and at all three concentrations of copper treatment (Fig. 5).

Multivariate analysis

Principal component (PCA) and hierarchical cluster analysis of all the biomarker reactions showed that the various treatments had a detrimental effect on the digestive cells of both mussels and periwinkles (Fig. 6, 7 & 8). Analysis of similarity showed that these clusters were significantly different (ANOSIM, $p \leq 0.001$); and clear separation of the effects of different treatments was apparent in the PCA and Cluster plots (Fig. 6, 7 & 8), and particularly for the periwinkles (Fig. 8). Regression analysis (Scatter Plot matrices, not shown) of the mussel biomarker data for the four most toxic treatments (i.e., chlorpyrifos, copper, fluoranthene & phenanthrene) indicated that LMS, was inversely correlated with lipofuscin, lysosomal lipid and protein carbonyls; and that lipofuscin was correlated with lysosomal lipid, except for the phenanthrene treatment, and protein carbonyls (Table 3). However, lysosomal lipid and protein carbonyls were not correlated (Table 3).

When all chemical treatments were analysed together for both species of mollusc, all four biomarkers were strongly correlated ($p \leq 0.001$) with the first Principal Components (Table 4).

Discussion

Indices of oxidative stress, cell injury and dysfunctional autophagy were assessed in both species of mollusc (i.e., lysosomal membrane stability, lipofuscin, protein carbonyls, and fatty change involving lysosomal accumulation of lipid [triglyceride] or lipidosis). Evidence of oxidative stress, based on the elevation of lipofuscin and protein carbonyls, was found for all compounds tested; with chlorpyrifos being the most toxic to both species (Sohal & Brunk, 1989, Sforzini et al., 2018; Shaw et al., 2011). Dysfunctional autophagy was induced by all of the compounds tested in both species, except for atrazine in mussels. Furthermore, dysfunctional autophagy was characterised by reduced lysosomal membrane integrity, increased lipofuscin or lipofuscinosis (indicative of oxidative stress) and increased lysosomal lipid or lipidosis (Moore et al., 2006a, 2007b; Terman & Brunk, 2002). This failure of normal autophagy was generally associated with oxidative stress (Moore et al., 2006b, 2007a, b, 2008).

All of the chemicals tested in this study induced some degree of oxidative stress (Table 2). ROS can damage lipoprotein membranes, and cellular proteins producing protein carbonyls and other oxidative products (Shaw et al., 2011; Sforzini et al., 2018). The damaged proteins and membranes are normally removed by autophagy; however, if the level of intracellular damage becomes excessive due to severe oxidative stress, then the autophagic processes are overwhelmed and become dysfunctional (Fig. 9). Lipofuscin build-up as a result of lipid peroxidation of autophagocytosed lipoprotein membranes (e.g., mitochondria and endoplasmic reticulum) is an effective biomarker for moderate to severe oxidative stress. However, lipofuscin, long thought of as an inert waste product of “cellular housekeeping”, is an effective generator of ROS due to Fenton reactions mediated by lipofuscin-bound iron, thereby, inhibiting lysosomal degradation (Grune et al., 2004; Terman & Brunk, 2004). The inference is that abnormal accumulation of lipofuscin in autolysosomes (i.e., lipofuscinosis) will result in excessive ROS production and oxidative stress (Fig. 9). ROS generation *in vivo* hepatopancreatic digestive cells has been demonstrated by Winston et al. (1991), indicating that there is a highly reactive oxidative intra-lysosomal environment in these cells (Terman & Brunk, 2002).

Fatty change is often a cellular pathological feature of a number of diseases including those resulting from exposure to a variety of organic xenobiotics (Fig. 9; Klaunig et al.,

2018). However, somewhat paradoxically starvation can also induce fatty change in mammals (Kneeman et al., 2012; Ohama et al., 1994), although there is no evidence for this pathological reaction in molluscs (Moore et al., unpublished data). This excess cytoplasmic lipid (triglyceride) can be autophagocytosed (lipophagy) and accumulates in autolysosomes: a condition known as lipidosis and effective autophagic degradation of intracellular material is inhibited by fatty change (Cingolani & Czaja, 2016; Koukouzika et al., 2009; Moore, 1988; Moore et al., 2007b; Ward et al., 2016; Yan et al., 2017).

The overall consequence is that oxidative stress results in reduced food uptake by inhibition of endocytosis, and augmented autophagy of damaged organelles, lipoprotein membranes and proteins (Fig.9; Flinn & Backer, 2010; Han & Wang, 2018; Sforzini et al., 2018). As the severity of oxidative stress increases, normal lysosomal and autophagic function is dysregulated, with reduced lysosomal membrane stability, intralysosomal build-up of triglyceride, phospholipid and lipofuscin; and further generation of ROS from the lipofuscin (Moore et al., 2006a, 2007b; Terman & Brunk, 2002).

This pathological syndrome of oxidative stress-linked dysfunctional autophagy is a major contributor to programmed cell death (PCD; Fig. 9), probably mediated by both apoptosis (PCD Type 1) and autophagic cell death (PCD Type 2) (Cuervo, 2008; Das et al., 2012; Lowe, 1988; Shimizu et al., 2014). The consequences for the animal will be digestive gland tissue atrophy as described by Lowe (1988), loss of fecundity and overall functional deterioration leading to death (Bayne et al., 1978; Lowe et al., 1982).

PAHs are known to accumulate in molluscan digestive cell lysosomes and cause damage to the membrane (Moore et al., 2004, 2006a, 2007a, b; Sforzini et al., 2018). Moore (1988) reported enlarged lysosomes, lipidosis, lipofuscinosis and a large reduction in lysosomal stability in periwinkles exposed to PAHs and other contaminants; and Lowe et al. (2006) also saw a reduction in lysosomal membrane stability in periwinkles exposed to 2 μ M fluoranthene for 5 days. Lysosomal membrane disruption may also result from the ability of PAHs, due to their lipophilicity, to penetrate and incorporate phenanthrene and fluoranthene into phospholipid membranes resulting in increased membrane lipid unsaturation and hydrophobicity (Nelson et al., 1990).

Furthermore, PAHs can be biotransformed in mussels by cytochromes P450 (a large family of proteins that biotransform exogenous and endogenous molecules) and hydroperoxides (Garcia Martinez, Livingstone, 1995; Lemaire et al., 1993). These hydroperoxides can catalyse PAH metabolism, forming cation radicals which can also bind to DNA and other macromolecules (Livingstone et al. 1990).

Chlorpyrifos and malathion are both known to induce oxidative stress in molluscs, and this reaction was associated with lysosomal injury and autophagic dysfunction, particularly with chlorpyrifos treatment in mussels and periwinkles (Canesi et al., 2011; Khalil, 2015; Livingstone, 2003). Oxidative damage as a result of malathion exposure has been reported in the freshwater snail *Stagnicola* sp., including elevation of MDA (Martinez-Tabche et al., 2002). Periwinkles were not treated with malathion.

Atrazine can induce oxidative stress in Pacific oysters (*Crassostrea gigas*), and some evidence for oxidative stress was observed in treated mussels (Table 2; Lee et al., 2017). However, this was limited to increased protein carbonyls and lysosomal destabilisation; and there was no evidence for dysfunction of autophagy (Table 1).

Copper accumulates in mussel lysosomes and probably exerts its toxicity by ROS attack on lysosomal membranes with subsequent reduction in membrane stability (Ringwood et al., 1998; Shepard & Bradley, 2000). However, in this study lysosomal stability did not prove to be more sensitive than induction of either lipofuscin, or protein carbonyls in either mussel or snails (Table 2). Elevated mussel lipofuscin and protein carbonyls, and reduced lysosomal membrane stability, were seen only in the 10 μM exposure. No elevated lipofuscin was seen in any periwinkle copper treatment (Table 2; Fig. 5). However increased protein carbonyl formation was detected in both the 0.1 μM and 1 μM exposures; and lysosome stability was seen to decrease only in the 10 μM treatment.

LAS, in common with other surfactants, has a strong affinity for sediments and it is thus postulated that filter feeders may have increased vulnerability to its toxic effects (Da Ros et al., 1995; Sanderson et al., 2006). However, LAS was only found to exert a free radical mediated toxic effect at the highest exposure concentration of 10 μM in this study (Fig. 1-4), suggesting that it is far less toxic than all the other compounds assessed in

the study, excepting atrazine. LAS probably exerts its toxic effect through the disruption of biological membranes via intercalation into the membrane bilayer. This can result in the solubilisation and substitution of the component proteins and lipids consequently disrupting membrane functions such as endocytosis and phagocytosis (Jackson et al. 1977). These observations suggest that the reduction of lysosomal membrane stability seen within this study may also result from LAS intercalation as well as ROS activity, as shown by the elevation of protein carbonyls (Table 2; Fig. 4). However, the absence of any increase (or even reduction) of lipofuscin indicated that oxidative stress was probably limited to the 10 μ M LAS treatment (Table 2; Fig. 1).

In summary, the patterns of toxic cell pathological reactions were very similar between mussel and periwinkle as previously demonstrated (Moore, 1988; Moore et al., 1987a, b). However, the snails were generally more susceptible to the toxic effects of chlorpyrifos and copper, which agrees with previous work demonstrating the robustness of mussels (*M. edulis*), compared to the common limpet (*Patella vulgata*) and crab (*Carcinus maenas*), on exposure to copper (Brown et al. 2004); and also the mussel *Amblema plicata*, compared to the oyster *Crassostrea virginica*, following exposure to chlorpyrifos (Borthwick et al. 1981; Doran et al. 2001). The main difference between the two test species in this investigation was that evidence for fatty change and lipidoses was more pronounced in the snails (see Table 2; Fig. 5).

Principal component analysis (PCA) is an effective method for integrating biomarker data for lysosomal pathology and oxidative stress into a "health status space", reducing the multi-dimensionality of the problem to a simple two dimensional representation (Allen and Moore, 2004; Chatfield and Collins, 1980). PCA is commonly used as a cluster analysis tool and effectively captures the variability in a dataset in terms of principal components. Previously PCA has facilitated modelling the integrated responses of multiple biomarkers in the context of "health status space" (Allen and Moore, 2004; Moore et al., 2006a, Sforzini et al., 2015, 2017, 2018). These models have shown that there is a strong direct relationship between LMS, as an indicator of cellular health, and the first principal components for the combined biomarker responses (Fig. 6, 7 & 8; Table 4; Allen & Moore, 2004; Moore et al., 2006a; Sforzini et al., 2018). The other biomarkers (lipofuscin, lysosomal lipid & protein carbonyls) are inversely correlated with the first principal components (Table 4).

Previous PCA and cluster analysis, which does not integrate the various biomarkers in a functionally meaningful way, was previously employed as the first stage in developing numerical and network models for environmental impact on the health of sentinel animals such as mussels and earthworms (Allen & McVeigh, 2004; Allen & Moore, 2004; Moore et al., 2015; Sforzini et al., 2016, 2017, 2018). Network models particularly, encapsulate the cellular physiological processes that enable the construction of a logical functional framework through the interconnections between the biomarker data; and, such models have repeatedly demonstrated the importance and utility of the set of biomarkers used in this investigation (Figs. 6, 7 & 8). The main output from the network models is a measure of system complexity (connectance %) and this is very strongly correlated with the first principal components and lysosomal membrane stability (LMS) as measures of functional integrity. Consequently, in this investigation, the first principal component is considered to be an effective functionally integrated representative index of “health status” (Moore et al., 2006a, 2007b; Sforzini et al., 2015, 2017, 2018).

A conceptual mechanistic model for stress reactions in molluscan hepatopancreatic digestive cells related to lysosomal functions autophagy has been developed to explain the findings from this investigation and the links between reactive oxygen species (ROS) generation, oxidative stress and autophagy (Fig. 9). The model also draws on previous studies (Moore et al., 2006a, 2007b; Shaw et al., 2011), including the effects of benz[a]pyrene on the mTOR (mechanistic target for rapamycin) cell signalling system (Sforzini et al., 2018). mTOR complex 1 (mTORC1) is one of the key controlling foci in the cellular regulatory network, where it regulates many aspects of cell growth. mTORC1 specifically regulates lysosomal membrane stability (permeability), lipogenesis and endocytosis; while inhibition by nutrient stress or oxidative stress triggers augmented physiological lysosomal autophagy (Flinn & Backer, 2010; Han & Wang, 2018; Laplante & Sabatini, 2012; Moore et al., 2015; Tan & Miyamoto, 2016). The model describes the interactive relationships between ROS, oxidative stress, mTORC1 inhibition, endocytosis, augmented physiological autophagy, lysosomal membrane stability, lipogenesis, fatty change, lysosomal lipidosis, lipofuscin generation, lysosomal lipofuscinosis, dysfunctional autophagy and programmed cell death (PCD Types 1 & 2) and digestive gland tubule tissue atrophy (Lowe, 1988). The mechanistic links between

these various pathological reactions have been described previously using quantitative network models for mussels and periwinkles (Moore et al., 2015; Sforzini et al., 2018).

Conclusions

Despite the diverse array of chemicals (i.e., PAHs, organophosphate insecticides, herbicide, transition metal and surfactant) used within this investigation, all have demonstrated a common initial mechanism of toxicity in the two test species. Oxidative stress, assessed via products of damage, appears to be a useful non-specific measurement of cellular perturbation. Lysosomal and autophagic dysregulation involving fatty change and lipid accumulation within the lysosomes of digestive cells also appears to be a useful integrated indicator of general chemical-induced stress as confirmed by previous work (Moore 1988; Domouhtsidou et al. 2001; Sforzini et al., 2018).

The toxic effects of the majority of compounds used within this study tended to be more prominent at the higher treatment concentrations (i.e., $\geq 1 \mu\text{M}$), and so, perhaps less environmentally relevant. However, animals were only exposed for 7 days; and much, if not most, of aquatic pollutant toxicity is chronic in nature. Consequently, the detrimental impact of exposure to these contaminants, at even the lowest levels used within this investigation, is likely to increase in severity over time.

The loss of normal and augmented autophagic function in the hepatopancreatic digestive cells, as a result of autophagic dysregulation, will have profound effects on the physiology of the mussels and periwinkles. The hepatopancreas or digestive gland is the major organ for digestion, assimilation of nutrients and storage of energy reserves (i.e. glycogen and lipids); and detoxication of toxic metals and organic xenobiotics (Moore et al., 2006a, 2007b). As such, its normal and physiologically augmented autophagic functions are essential for the wellbeing of the whole animal; and if these become dysfunctional then the health of the animal declines as demonstrated by the related decline in physiological scope for growth (Moore et al., 2006a).

Failure of normal and physiologically augmented autophagic function as a pathological reaction to chemically induced stress appears to be a widespread phenomenon in many eukaryotic species, including molluscs, annelids and mammals, perhaps indicating that this type of reaction is generic. Evidence for the generic nature of this pathological

reaction, is supported by the observations from the present investigation and builds on previous studies (Cuervo, 2004, 2008). Dysfunctional autophagy is characteristic of a number of animal and human diseases, including neurodegenerative diseases, fibromyalgia, ocular pathologies, cardiovascular disease and obesity related conditions (Cajaraville et al., 1995; Chen et al., 2012; Colacurcio et al 2018; Cuervo, 2004; Domouhtsidou et al. 2001; Jiang & Mizushima, 2014; Moore et al., 2006a, 2007b; Namkoong et al., 2018; Nixon, 2013; Numan et al., 2015; Oezel et al., 2016; Sforzini et al., 2018; Yan et al., 2017). Some of these disease conditions have been linked to uptake of harmful nanoscale materials derived from road traffic (Bai et., 2016; Chen et al., 2016; Numan et al., 2015).

Acknowledgements

This work was part of the PREDICT 2 project jointly supported by the UK Department for Environment, Food and Rural Affairs (Defra, UK) (contract number AE1136) and the Natural Environment Research Council (NERC UK). There are no conflicts of interest.

References

- Alamdari, D.H., Kostidou, E., Paletas, K., Sarigianni, M., Konstas, A.G.P., Karapiperidou, A., Koliakos, G., 2005. High sensitivity enzyme-linked immunosorbent assay (ELISA) method for measuring protein carbonyl in samples with low amounts of protein. *Free Radical Biology & Medicine* 39, 1362–1367.
- Allen, J.I., Moore, M.N., 2004. Environmental prognostics: is the current use of biomarkers appropriate for environmental risk evaluation. *Marine Environmental Research* 58, 227-232.
- Bai, R., Guan, L., Zhang, W., Xu, J., Rui, W., Zhang, F., Ding, W. (2016). Comparative study of the effects of PM1-induced oxidative stress on autophagy and surfactant protein B and C expressions in lung alveolar type II epithelial MLE-12 cells. *Biochimica et Biophysica Acta* 1860, 2782–2792.
- Bayne, B.L., Holland, D.L., Moore, M.N., Lowe, D.M., Widdows, J., 1978. Further studies on the effects of stress in the adult on the eggs of *Mytilus edulis*. *Journal of the Marine Biological Association U.K.* 58, 825-841.
- Borthwick, P.W., Walsh, G.E., 1981. Initial Toxicological Assessment of Ambush, Bolero, Bux, Dursban, Fentripanil, Larvin and Pydrin Static Acute Toxicity Tests with selected Estuarine Algae, Invertebrates and Fish. In: U.S. Environmental Protection Agency, Washington, D.C.,
- Boya, P., 2012. Lysosomal function and dysfunction: mechanism and disease. *Antioxidant & Redox Signaling* 17, 766-774.
- Brown, R.J., Galloway, T.S., Lowe, D., Browne, M.A., Dissanayake, A., Jones, M.B., Depledge, M.H., 2004. Differential sensitivity of three marine invertebrates to copper assessed using multiple biomarkers. *Aquatic Toxicology* 66, 262-278.
- Cajaraville, M.P., Abascal, I., Etxeberría, M., Marigomez, I., 1995. Lysosomes as cellular markers of environmental pollution: time- and dose-dependent responses of the

- digestive lysosomal system of mussels after petroleum hydrocarbon exposure. *Environmental Toxicology and Water Quality* 10, 1-8.
- Cassee, F.R., Groten, J., van Bladeren, P.J., Feron, V.J., 2008. Toxicological evaluation and risk assessment of chemical mixtures. *Critical Reviews in Toxicology* 28, 73-101.
- Canesi L, Negri A, Barmo C, Banni M, Gallo G, Viarengo, A. Dondero, F., 2011. The organophosphate chlorpyrifos interferes with the responses to 17 β -estradiol in the digestive gland of the marine mussel *Mytilus galloprovincialis*. *PLoS ONE* 6(5): e19803. doi:10.1371/journal.pone.0019803
- Chatfield, C., Collins, A. J., 1980. Introduction to multivariate analysis. London: Chapman and Hall.
- Chen, S., Zhang, X., Song, L., Le, W. 2012. Autophagy dysregulation in amyotrophic lateral sclerosis. *Brain Pathology* 22, 110–116.
- Chen, Z.-H., Wu, Y.-F., Wang, P.-L., Wu, Y.-P., Li, Zhao, Y., Zhou, J.-S., Zhu, C., Cao, C., Mao, Y.-Y., Xu, F., Wang, B.-B., Cormier, S.A., Ying, S.-M., Li, W., Shen, H.-H., 2016. Autophagy is essential for ultrafine particle-induced inflammation and mucus hyperproduction in airway epithelium. *Autophagy* 12, 297–311.
- Cingolani, F., Czaja, M.J., 2016. Regulation and functions of autophagic lipolysis. *Trends in Endocrinological Metabolism* 27, 696-705.
- Clarke, K.R., 1999. Non-metric multivariate analysis in community-level ecotoxicology. *Environmental & Toxicological Chemistry* 18, 117-127.
- Clarke, K.R., Warwick, R.M., 2001. Change in marine communities: an approach to statistical analysis and interpretation. PRIMER-e, Plymouth, UK.
- Colacurcio, D.J., Pensalfini, A., Jiang, Y., Nixon, R.A., 2018. Dysfunction of autophagy and endosomal-lysosomal pathways: roles in pathogenesis of Down syndrome and Alzheimer's disease. *Free Radical Biology & Medicine* 114, 40-51.
- Cuervo, A.M., 2004. Autophagy: in sickness and in health. *TRENDS Cell Biol.* 14, 70-77.
- Cuervo, A.M., 2008. Autophagy and aging: Keeping that old broom working. *Trends in Genetics* 24, 604–612.
- Da Ros, L., Nasci, C., Campesan, G., Sartorello, P., Stocco, G., Menetto, A., 1995. Effects of linear alkylbenzene sulphonate (LAS) and cadmium in the digestive gland of mussel, *Mytilus* sp. *Marine Environmental Research* 39, 321-324.
- Das, G., Shrivage, B. V., & Baehrecke, E. H., 2012. Regulation and function of of autophagy during cell survival and cell death. *Cold Spring Harbor perspectives in biology*, 4(6), 10.1101/cshperspect.a008813 a008813. doi:10.1101/cshperspect.a008813
- Dimitriadis, V.K., Domouhtsidou, G.P., Cajaraville, M.P., 2004. Cytochemical and histochemical aspects of the digestive gland cells of the mussel *Mytilus galloprovincialis* (L.) in relation to function. *Journal of Molecular Histology* 35, 501-509.
- Domouhtsidou, G.P., Dimitriadis, V.K., 2001. Lysosomal and lipid alterations in the digestive gland of mussels, *Mytilus galloprovincialis* (L.) as biomarkers of environmental stress. *Environmental Pollution* 115, 123-137.
- Doran, W.J., Cope, W.G., Rada, R., Sandheinrich, M.B., 2001. Acetylcholinesterase inhibition in the threeridge mussel (*Amblema plicata*) by chlorpyrifos: implications for biomonitoring. *Ecotoxicology and Environmental Safety* 49, 91-98.
- Flinn, R.J., Backer, J.M., 2010. mTORC1 signals from late endosomes: taking a TOR of the endocytic system. *Cell Cycle*, 9, 1869-1870.
- Frank, J., Pompella, A., Biesalski, H.K., 2000. Histochemical visualization of oxidant stress. *Free Radical Biology & Medicine* 29, 1096–1105.

- Garcia Martinez, P., Livingstone, D.R., 1995. Benzo[a]pyrene-dione-stimulated oxyradical production by microsomes of digestive gland of the common mussel (*Mytilus edulis* L.). *Toxicology And Applied Pharmacology* 131, 332-341.
- Grune, T., Jung, T., Merker, K., Davies, K.J.A., 2004. Decreased proteolysis caused by protein aggregates, inclusion bodies, plaques, lipofuscin, ceroid, and "aggresomes" during oxidative stress, ageing and disease. *International Journal of Biochemistry & Cell Biology* 36, 2519-2530.
- Hamed, M.A., Emara, A.M., 2006. Marine molluscs as biomonitors for heavy metal levels in the Gulf of Suez, Red Sea. *Journal of Marine Systems* 60, 220-234.
- Han, J., Wang, Y., 2018. mTORC1 signaling in hepatic lipid metabolism. *Protein & Cell* 9, 145–151.
- Jackson, W.F., Fromm, P.O., 1977. Effects of detergent on flux of tritiated water into isolated perfused gills of rainbow trout. *Comparative Biochemistry and Physiology* 58C, 167-171.
- Jiang, P., Mizushima, N. 2014. Autophagy and human diseases. *Cell Res.* 24, 69–79.
- Kelly, C.A., Law, R.J., Emerson, H.S., 2000. Methods for analysis of hydrocarbons and polycyclic aromatic hydrocarbons (PAH) in marine samples. *Aquatic Environment Protection - Analytical Methods*, No. 12. Centre for Environment, Fisheries and Aquaculture Science, Lowestoft.
- Khalil, A.M., 2015. Toxicological effects and oxidative stress responses in freshwater snail, *Lanistes carinatus*, following exposure to chlorpyrifos. *Ecotoxicology & Environmental Safety* 116, 137–142.
- Klaunig, J.E., Li, X., Wang, Z., 2018. Role of xenobiotics in the induction and progression of fatty liver disease. *Toxicology Research (Camb)* 7, 664-680.
- Klionsky, D.J. Abdelmohsen. K., Abe, A., Abedin, M.J., Abeliovich, H., Acevedo Arozana, A., et al., 2016. Guidelines for the use and interpretation of assays for monitoring autophagy (3rd edition). *Autophagy* 12,1-222.
- Kneeman, J. M., Misdraji, J., Corey, K. E., 2012. Secondary causes of nonalcoholic fatty liver disease. *Therapeutic Advances in Gastroenterology* 5, 199–207.
- Koukouzika, N., Raftopoulou, E.K., Dimitriadis, V.K., 2009. Seasonal differences of lysosomal, lipid and lipofuscin parameters in the digestive gland of the mussel *Mytilus galloprovincialis*. *Journal of Molluscan Studies* 75, 261–267.
- Langston, W.J., G. Burt & N. Pope, 1999. Bioavailability of metals in sediments of the dogger bank (central north sea): a mesocosm study. *Estuarine, Coastal and Shelf Science* 48: 519-540.
- Laplante, M., Sabatini, D.M., 2012. mTOR signaling in growth control and disease. *Cell* 149, 274-293.
- Law, R.J., Kelly, C.A., Nicholson, M.D., 1999. Polycyclic aromatic hydrocarbons (PAH) in shellfish affected by the Sea Empress oil spill in Wales in 1996. *Polycyclic Aromatic Compounds*, 17, 229-239.
- LeBlanc, G.A., Olmstead, A.W., 2004. Evaluating the toxicity of chemical mixtures. *Environmental Health Perspectives* 112, A729–A730.
- Lee, D.-H., Rhee, Y.-J., Choi, K.-S., Nam, S.-E., Eom, H.-J., Rhee, J.-S., 2017. Sublethal concentrations of atrazine promote molecular and biochemical changes in the digestive gland of the Pacific oyster *Crassostrea gigas*. *Toxicology and Environmental Health Sciences* 9, 50-58.
- Lemaire, P., Den Besten, P.J., O'Hara, S.C.M., Livingstone, D.R., 1993. Comparative metabolism of benzo[a]pyrene by microsomes of hepatopancreas of the shore crab *CArcinus maenas* L. and digestive gland of the common mussel *Mytilus edulis* L. *Polycyclic Aromatic Compounds* 3, 1134-1138.

- Livingstone, D.R., 2003. Oxidative stress in aquatic organisms in relation to pollution and aquaculture. *Revue de Médecine Vétérinaire*, 154, 427-430.
- Livingstone, D.R., Martinez, P.G., Michel, X., Narbonne, J.F., O'Hara, S.C.M., Ribera, D., Winston, G.W., 1990. Oxyradical production as a pollution-mediated mechanism of toxicity in the common mussel, *Mytilus edulis* L., and other molluscs. *Functional Ecology* 4, 415-424.
- Lowe, D.M., Moore, M.N., Bayne, B.L. 1982. Aspects of gametogenesis in the marine mussel *Mytilus edulis*. *Journal of the Marine Biological Association U.K.* 62, 133-145.
- Lowe, D.M., 1988. Alterations in the cellular structure of *Mytilus edulis* resulting from exposure to environmental contaminants under field and experimental conditions. *Marine Ecology Progress Series* 46, 91-100.
- Lowe, D.M., Moore, M.N., Readman, J.W., 2006. Pathological reactions and recovery of hepatopancreatic digestive cells from the marine snail *Littorina littorea* following exposure to a polycyclic aromatic hydrocarbon. *Marine Environmental Research* 61, 457-470.
- Moore, M.N., 1988. Cytochemical responses of the lysosomal system and NADPH-ferrihaemoprotein reductase in molluscan digestive cells to environmental and experimental exposure to xenobiotics. *Marine Ecology Progress Series* 46, 81-89.
- Moore, M.N., 2008. Autophagy as a second level protective process in conferring resistance to environmentally-induced oxidative stress. *Autophagy* 4, 254-256.
- Moore, M.N., 2010. Autophagy as a protective process in environmentally-induced oxidative stress. *Comparative Biochemistry & Physiology A - Molecular & Integrative Physiology* 157, S51.
- Moore, M.N., Allen, J.I., McVeigh, A., 2006a. Environmental prognostics: an integrated model supporting lysosomal stress responses as predictive biomarkers of animal health status. *Marine Environmental Research* 61, 278–304.
- Moore, M.N., Allen, J.I., McVeigh, A., Shaw, J., 2006b. Lysosomal and autophagic reactions as diagnostic and predictive indicators of environmental pollutant toxicity in aquatic animals. *Autophagy* 2, 217-220.
- Moore, M.N., Allen, J.I., Somerfield, P.J., 2007a. Autophagy: Role in surviving environmental stress. *Marine Environmental Research* 62, S420-S425.
- Moore, M.N., Koehler, A., Lowe, D. & Viarengo, A., 2008. Lysosomes and autophagy in aquatic animals. In: *Methods in Enzymology* (D.Klionsky, Ed), 451, 582-620. Academic Press/Elsevier, Burlington.
- Moore, M.N., Shaw, J.P., Ferrar Adams, D.R., Viarengo, A., 2015. Protective effect of fasting-induced autophagy and reduction of age-pigment in the hepatopancreatic cells of a marine snail. *Marine Environmental Research* 107, 35-44.
- Moore, M.N., Viarengo, A., Donkin, P., Hawkins, A.J.S., 2007b. Autophagic and lysosomal reactions to stress in the hepatopancreas of blue mussels. *Aquatic Toxicology* 84, 80-91.
- Moore, M.N., Wedderburn, J., Clarke, K.R., McFadzen, I., Lowe, D.M., Readman, J.W., 2018. Emergent synergistic lysosomal toxicity of chemical mixtures in molluscan blood cells (hemocytes). *Environmental Pollution* 235, 1006-1014.
- Namkoong, S., Cho, C. S., Semple, I., & Lee, J. H. (2018). Autophagy dysregulation and obesity-associated pathologies. *Molecules & Cells*, 41, 3–10.
- Nelson, A., Auffret, N., Borlakoglu, J.T., 1990. Interaction of hydrophobic organic compounds with mercury adsorbed dioleoylphosphatidylcholine monolayers. *Biochimica et Biophysica Acta* 1021, 205-216.
- Nixon, R.A. 2013. The role of autophagy in neurodegenerative disease. *Nature Medicine* 19, 983–997.

- Numan, M.S., Brown, J.P., Michou, L. (2015). Impact of air pollutants on oxidative stress in common autophagy-mediated aging diseases. *International Journal of Environmental Research & Public Health* 12, 2289-2305.
- Oezel, L., Then, H., Jung, A.L., Jabari, S., Bonaterra, G.A., Wisniewski, T.T., Önel, S.F., Ocker, M., Thieme, K., Kinscherf, R., Di Fazio, P., 2016. Fibromyalgia syndrome: metabolic and autophagic processes in intermittent cold stress mice. *Pharmacology Research Perspectives* 4(5):e00248. doi: 10.1002/prp2.248.
- Ohama, T., Matsuki, N., Saito, H., Tsukamoto, K., Kinoshita, M., Katsuragawa, K., Okazaki, S., Yamanaka, M., Teramoto, T., 1994. Effect of starving and refeeding on lipid metabolism in suncus. *Journal of Biochemistry* 115, 190-193.
- Readman, J.W., Fillmann, G., Tolosa, I., Bartocci, J., Villeneuve, J.-P., Cattini, C., Mee, L.D. (2002). Petroleum and PAH contamination of the Black Sea. *Marine Pollution Bulletin*, 44, 48-62.
- Ringwood, A.H., Conners, D.E., Di Novo, A., 1998. The effects of copper exposures on cellular responses in oysters. *Marine Environmental Research* 46, 591-595.
- Sanderson, H., Dyer, S.D., Price, B.B., Nielson, A.M., van Compernelle, R., Selby, M., Stanton, K., Evans, A., Ciarlo, M., Sedlak, R., 2006. Occurrence and weight-of-evidence risk assessment of alkyl sulphates, alkyl ethoxysulphates and linear alkylbenzene sulphonates (LAS) in river water and sediments. *Science of the Total Environment* 368, 695-712.
- Sforzini, S., Moore, M.N., Boeri, M., Bencivenga, M., Viarengo, A., 2015. Effects of PAHs and dioxins on the earthworm *Eisenia andrei*: a multivariate approach for biomarker interpretation. *Environmental Pollution* 196, 60-71.
- Sforzini, S., Moore, M.N., Mou, Z., Boeri, M., Banni, M., Viarengo, A., 2017. Mode of action of Cr(VI) in immunocytes of earthworms: Implications for animal health. *Ecotoxicology & Environmental Safety* 138, 298–308.
- Sforzini, S., Moore, M.N., Oliveri, C., Volta, A., Jha, A., Banni, M., Viarengo, A., 2018. Probable role of mTOR in autophagic and lysosomal reactions to environmental stressors in molluscs. *Aquatic Toxicology* 195, 114–128.
- Shaw, J.P., Dondero, F., Moore, M.N., Negri, A., Dagnino, A., Readman, J.W., Low, D.M., Frickers, P.E., Beesley, A., Thain, J.E., Viarengo, A., 2011. Integration of biochemical, histochemical and toxicogenomic indices for the assessment of health status of mussels from the Tamar Estuary, U.K.. *Marine Environmental Research* 72, 13-24.
- Shepard, J.L., Bradley, B.P., 2000. Protein expression signatures and lysosomal stability in *Mytilus edulis* exposed to graded copper concentrations. *Marine Environmental Research* 50, 457-463.
- Shimizu, H., Woodcock, S.A., Wilkin, M.B., Trubenová, B., Monk, N.A., Baron, M., 2014. Compensatory flux changes within an endocytic trafficking network maintain thermal robustness of notch signaling. *Cell* 157, 1160--1174.
- Smith, M. A., Sayre, L. M., Anderson, V. E., Harris, P. L. R., Beal, M. F., Kowall, N., Perry, G., 1998. Cytochemical demonstration of oxidative damage in alzheimer disease by immunochemical enhancement of the carbonyl reaction with 2,4-dinitrophenylhydrazine. *Journal of Histochemistry & Cytochemistry*, 46, 731–735.
- Sohal, R.S., Brunk, U.T., 1989. Lipofuscin as an indicator of oxidative stress and aging. *Advances in Experimental Medicine & Biology* 266, 17–29.
- Tan, V.P., Miyamoto, S., 2016. Nutrient-sensing mTORC1: Integration of metabolic and autophagic signals. *Journal of Molecular & Cellular Cardiology* 95, 31-41.
- Terman, A., Brunk, U.T., 2004. Lipofuscin. *The International Journal of Biochemistry & Cell Biology* 36, 1400-1404.

- Venier, P., Canova, S., 1996. Formation of DNA adducts in the gill tissue of *Mytilus galloprovincialis* treated with benzo[a]pyrene. *Aquatic Toxicology* 34, 119-133.
- Ward, C., Martinez-Lopez, N., Otten, E.G., Carroll, B., Maetzel, D., Singh, R., Sarkar, S., Korolchuk, V.I., 2016. Autophagy, lipophagy and lysosomal lipid storage disorders. *Biochimica et Biophysica Acta* 1861, 269-284.
- Winston, G.W., Moore, M.N., Straatsburg, I., Kirchin, M. (1991). Lysosomal stability in *Mytilus edulis* L.: potential as a biomarker of oxidative stress related to environmental contamination. *Archives of Environmental Contamination & Toxicology* 21, 401-408.
- Yan, S., Huda, N., Khambu, B., Yin, X.-M., 2017. Relevance of autophagy to fatty liver diseases and potential therapeutic applications. *Amino Acids* 49, 1965–1979.

Figure Legends

Fig. 1. Lipofuscin in digestive gland of mussels (4.8 – 5.2 cm) exposed to 0.1 μM , 1 μM and 10 μM of atrazine, chlorpyrifos, copper, fluoranthene, LAS, malathion and phenanthrene for 7 days. The carrier or vehicle control (VC) solvent was DMSO. Data is presented as the mean \pm 95 % CL; lipofuscin (absorbance).

Fig. 2. Lysosomal membrane stability (LMS - based on N-acetyl- β -hexosaminidase latency) in digestive gland of mussels (4.8 – 5.2 cm) exposed to 0.1 μM , 1 μM and 10 μM of atrazine, chlorpyrifos, copper, fluoranthene, LAS, malathion and phenanthrene for 7 days. The carrier or vehicle control (VC) solvent was DMSO. Data is presented as the mean \pm 95 % CL; LMS is shown in minutes.

Fig. 3. Neutral lipids (triglycerides) in digestive gland of mussels (4.8 – 5.2 cm) exposed to 0.1 μM , 1 μM and 10 μM of atrazine, chlorpyrifos, copper, fluoranthene, LAS, malathion and phenanthrene for 7 days. The carrier or vehicle control (VC) solvent was DMSO. Data is presented as the mean \pm 95 % CL; neutral lipids (absorbance).

Fig. 4. Protein carbonyls in digestive gland of mussels (4.8 – 5.2 cm) exposed to 0.1 μM , 1 μM and 10 μM of atrazine, chlorpyrifos, copper, fluoranthene, LAS, malathion and phenanthrene for 7 days. The carrier or vehicle control (VC) solvent was DMSO. Data is presented as the mean \pm 95 % CL; protein carbonyls (density).

Fig. 5. Lipofuscin, lysosomal membrane stability (based on β -glucuronidase latency), lysosomal lipids and protein carbonyls in digestive gland of periwinkles (2 – 2.5 cm) exposed to 0.1 μM , 1 μM and 10 μM of chlorpyrifos, copper and phenanthrene for 7 days. The carrier or vehicle control (VC) solvent was DMSO. Data is presented as the mean \pm 95 % CL.

Fig. 6. Combined principal component and cluster analysis (i.e., ellipsoid boundaries based on Euclidean distance) for all of the test compounds, based on the data for the four biomarkers in mussels. Vectors for the individual biomarkers are shown; and the large arrow indicates increasing cellular pathology. Exposure times are noted in key as 0 or 7 (days). PC1 and PC2 captured 44.5% and 24.3% of the variation respectively.

Fig. 7. Individual principal component analysis and cluster analysis (i.e., ellipsoid boundaries based on Euclidean distance) for each of the test compounds, based on the data for the four biomarkers in mussels. Vectors for the individual biomarkers are shown; and the large arrow indicates increasing cellular pathology. Exposure times are noted in key as 0 or 7 (days).

Fig. 8. Combined principal component analysis and cluster analysis (i.e., ellipsoid boundaries based on Euclidean distance) for all of the test compounds, based on the data for the four biomarkers in periwinkles. Vectors for the individual biomarkers are shown; and the large arrow indicates increasing cellular pathology. Exposure times are noted in key as 0 or 7 (days). PC1 and PC2 captured 54.8% and 22.4% of the variation respectively.

Fig. 9. Conceptual mechanistic model for the role of oxidative stress in dysregulation of autophagy and heterophagy in hepatopancreatic digestive cells. Processes outlined in narrow red are considered to be potentially adverse; and those outlined in thick red constitute cell injury and programmed cell death (PCD). mTORC1 is the mechanistic target for rapamycin complex 1 – a key component of the cellular signalling system. Dotted arrows indicates generic process, although not yet confirmed in molluscs.

Table 1. Table of water (Day 0) and tissue chemistry for mussel and periwinkle following 7 days exposure treatments to contaminant chemical concentrations of 0.1 μM , 1 μM and 10 μM .

Treatment		<i>Mussel</i>		<i>Periwinkle</i>	
		Water ($\mu\text{M/L}$)	Tissue ($\mu\text{g/g dry weight}$)	Water ($\mu\text{M/L}$)	Tissue ($\mu\text{g/g dry weight}$)
Atrazine	Control	0	-	-	-
	0.1 μM	0.029468	-	-	-
	1 μM	0.45563	-	-	-
	10 μM	3.557744	-	-	-
Chlorpyrifos	Control	0	-	0	-
	0.1 μM	0.018	-	0.002	-
	1 μM	0.068	-	0.056	-
	10 μM	0.685	-	0.621	-
Copper	Control	0.004	0.77	0.005	1.55
	0.1 μM	0.043	0.89	0.068	1.8
	1 μM	0.41	2.85	0.57	4.67
	10 μM	8.2	2.8	9.83	4.2
Fluoranthene	Control	0	0.3	-	-
	0.1 μM	0.022	39.2	-	-
	1 μM	0.810	833.6	-	-
	10 μM	5.073	4273.9	-	-
LAS	Control	0.09	-	-	-
	0.1 μM	0.3261	-	-	-
	1 μM	0.8098	-	-	-
	10 μM	4.2055	-	-	-
Malathion	Control	0	-	-	-
	0.1 μM	0.085	-	-	-
	1 μM	0.911	-	-	-
	10 μM	3.193	-	-	-
Phenanthrene	Control	-	8.69	0.001	0.02
	0.1 μM	-	85.72	0.022	4.26
	1 μM	-	870.53	0.184	86.52
	10 μM	-	2061.13	1.297	605.68

Water chemistry results are presented as $\mu\text{M/L}$. Tissue chemistry results are presented as $\mu\text{g/g dry weight}$. Chlorpyrifos, LAS and malathion cannot be quantified in tissue; *L. littorea* was not exposed to atrazine, fluoranthene, LAS or malathion.

Table 2. Summary of biomarker responses and the inferred cellular pathological reactions in mussel and periwinkle digestive cells. Mussels were exposed to atrazine, chlorpyrifos, copper, fluoranthene, LAS, malathion and phenanthrene, and periwinkles were exposed to chlorpyrifos, copper and phenanthrene at concentrations of 0.1 μM , 1 μM and 10 μM for 7 days.

Treatment	Lysosomal lipofuscin	Lysosomal stability	Lysosomal lipids	Protein carbonyls	Oxidative stress	Dysfunctional autophagy
Atrazine						
0.1 μM						
1 μM		↓	↓	↑	✓	
10 μM		↓	↓	↑	✓	
Chlorpyrifos						
0.1 μM		↓↓	↑↑			✓✓
1 μM	↑	↓↓	↑↑	↑	✓	✓✓
10 μM	↑↑	↓↓	↑↑	↑↑	✓✓	✓✓
Copper						
0.1 μM			↑↑	↑		
1 μM			↑	↑↑		
10 μM	↑	↓↓	↑	↑↑	✓✓	✓✓
Fluoranthene						
0.1 μM	↑				?	
1 μM	↑	↓	↑	↑	✓	✓
10 μM	↑	↓		↑	✓	✓
LAS						
0.1 μM				↑	?	
1 μM				↑	?	
10 μM	↓	↓	↑	↑	✓	✓
Malathion						
0.1 μM	↑				?	
1 μM		↓	↓			
10 μM	↑	↓	↓	↑	✓	✓
Phenanthrene						
0.1 μM	↑↑				??	
1 μM	↑↑	↓↓	↑	↑	✓✓	✓✓
10 μM	↑↑	↓↓	↑	↑↑	✓✓	✓✓

↑ & ↓ represent significant ($p \leq 0.05$) increases and decreases in mussels; and ↑ & ↓ represent significant ($p \leq 0.05$) increases and decreases in periwinkles, from the day 7 control (or carrier

control, where applicable); ✓ - represents the presence of oxidative stress and dysfunctional autophagy in mussels; ✓ - represents the presence of oxidative stress and dysfunctional autophagy in periwinkles; ? - represents possible mild oxidative stress in mussels; and ? - represents possible mild oxidative stress in periwinkles.

Journal Pre-proof

Table 3. Correlations between biomarkers from regression matrices for fluoranthene, phenanthrene, chlorpyrifos and copper treatments in mussels.

Biomarker	LMS	Lipofuscin	Lipid
Fluoranthene			
<i>Lipofuscin</i>	-0.689***		
<i>Lipid</i>	-0.406**	0.497***	
<i>Protein carbonyls</i>	-0.567***	0.382**	0.159
Phenanthrene			
<i>Lipofuscin</i>	-0.632***		
<i>Lipid</i>	-0.254*	0.081	
<i>Protein carbonyls</i>	-0.510***	0.323**	0.237
Chlorpyrifos			
<i>Lipofuscin</i>	-0.286*		
<i>Lipid</i>	-0.761***	0.420***	
<i>Protein carbonyls</i>	-0.421***	0.289**	0.368
Copper			
<i>Lipofuscin</i>	-0.689***		
<i>Lipid</i>	-0.406**	0.497***	
<i>Protein carbonyls</i>	-0.567***	0.382**	0.159

Values are Pearson's Coefficient of Correlation R. *p < 0.05; **p < 0.01; ***p < 0.001; 58df.

Table 4. Correlation coefficients for the first Principal Component derived from all treatments as a “measure of health status” versus the individual biomarkers for mussels and periwinkles.

First Principal Component	<i>Lysosomal Membrane Stability</i>	<i>Lipofuscin</i>	<i>Lipid</i>	<i>Protein Carbonyls</i>
<i>PC 1 - Mussels</i>	0.71***	-0.60***	-0.59***	-0.75***
<i>PC 1 - Littorinids</i>	0.79***	-0.64***	-0.79***	-0.75***

Values are Pearson's Coefficient of Correlation R. Mussels - n = 400; Periwinkles – n = 170; *** p ≤ 0.001

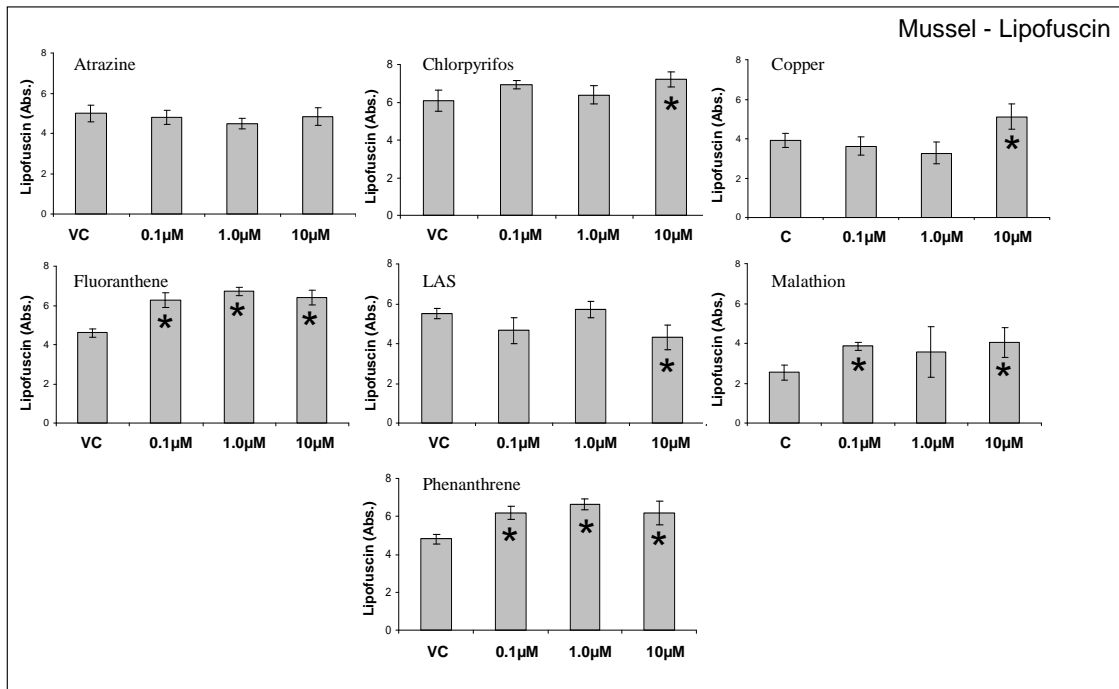


Fig. 1. Lipofuscin in digestive gland of mussels (4.8 – 5.2 cm) exposed to 0.1 μM, 1 μM and 10 μM of atrazine, chlorpyrifos, copper, fluoranthene, LAS, malathion and phenanthrene for 7 days. The carrier or vehicle control (VC) solvent was DMSO. Data is presented as the mean ± 95 % CL; lipofuscin (absorbance).

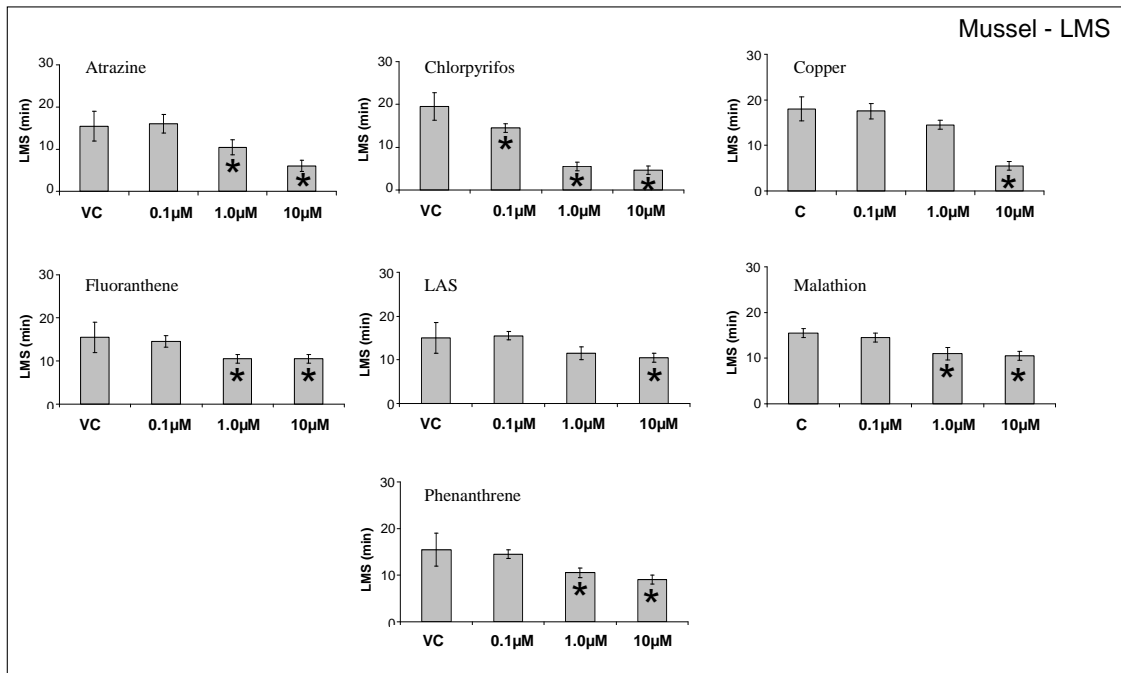


Fig. 2. Lysosomal membrane stability (LMS - based on N-acetyl- β -hexosaminidase latency) in digestive gland of mussels (4.8 – 5.2 cm) exposed to 0.1 μ M, 1 μ M and 10 μ M of atrazine, chlorpyrifos, copper, fluoranthene, LAS, malathion and phenanthrene for 7 days. The carrier or vehicle control (VC) solvent was DMSO. Data is presented as the mean \pm 95 % CL; LMS is shown in minutes.

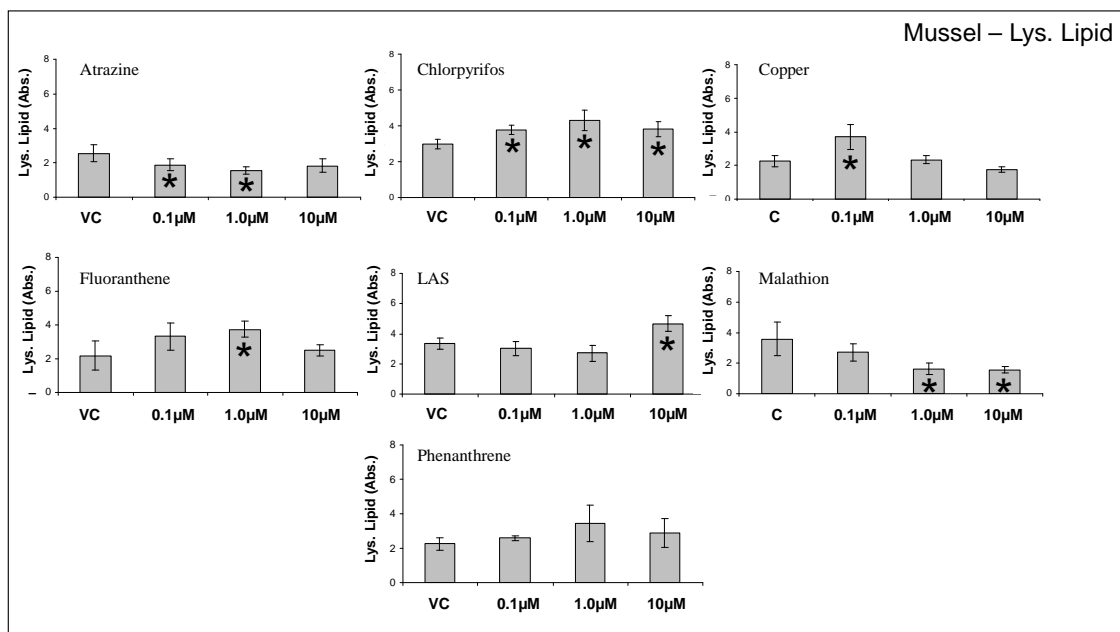


Fig. 3. Neutral lipids in digestive gland of mussels (4.8 – 5.2 cm) exposed to 0.1 μM, 1 μM and 10 μM of atrazine, chlorpyrifos, copper, fluoranthene, LAS, malathion and phenanthrene for 7 days. The carrier or vehicle control (VC) solvent was DMSO. Data is presented as the mean ± 95 % CL; neutral lipids (absorbance).

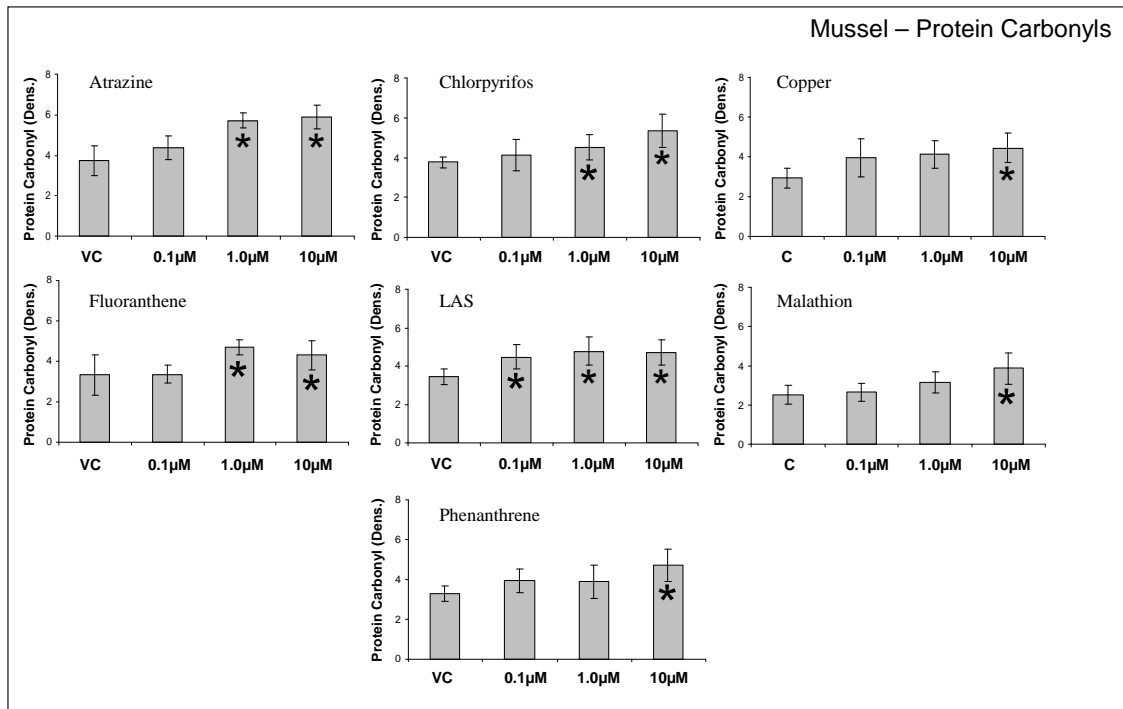


Fig. 4. Protein carbonyls in digestive gland of mussels (4.8 – 5.2 cm) exposed to 0.1 μM, 1 μM and 10 μM of atrazine, chlorpyrifos, copper, fluoranthene, LAS, malathion and phenanthrene for 7 days. The carrier or vehicle control (VC) solvent was DMSO. Data is presented as the mean ± 95 % CL; protein carbonyls (density).

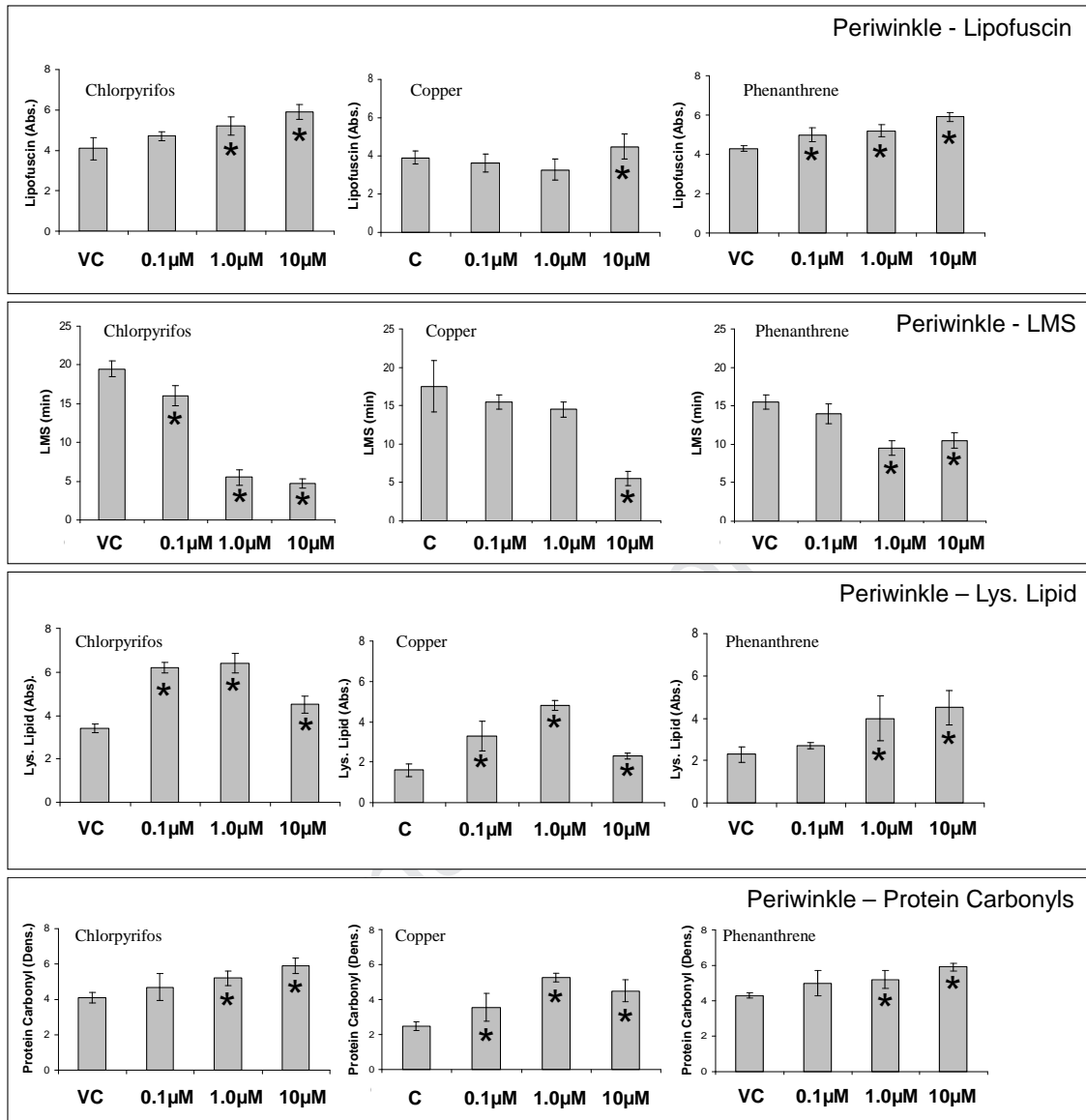


Fig. 5. Lipofuscin, lysosomal membrane stability (based on β -glucuronidase latency), lysosomal lipids and protein carbonyls in digestive gland of periwinkles (2 – 2.5 cm) exposed to 0.1 μ M, 1 μ M and 10 μ M of chlorpyrifos, copper and phenanthrene for 7 days. The carrier or vehicle control (VC) solvent was DMSO. Data is presented as the mean \pm 95 % CL.

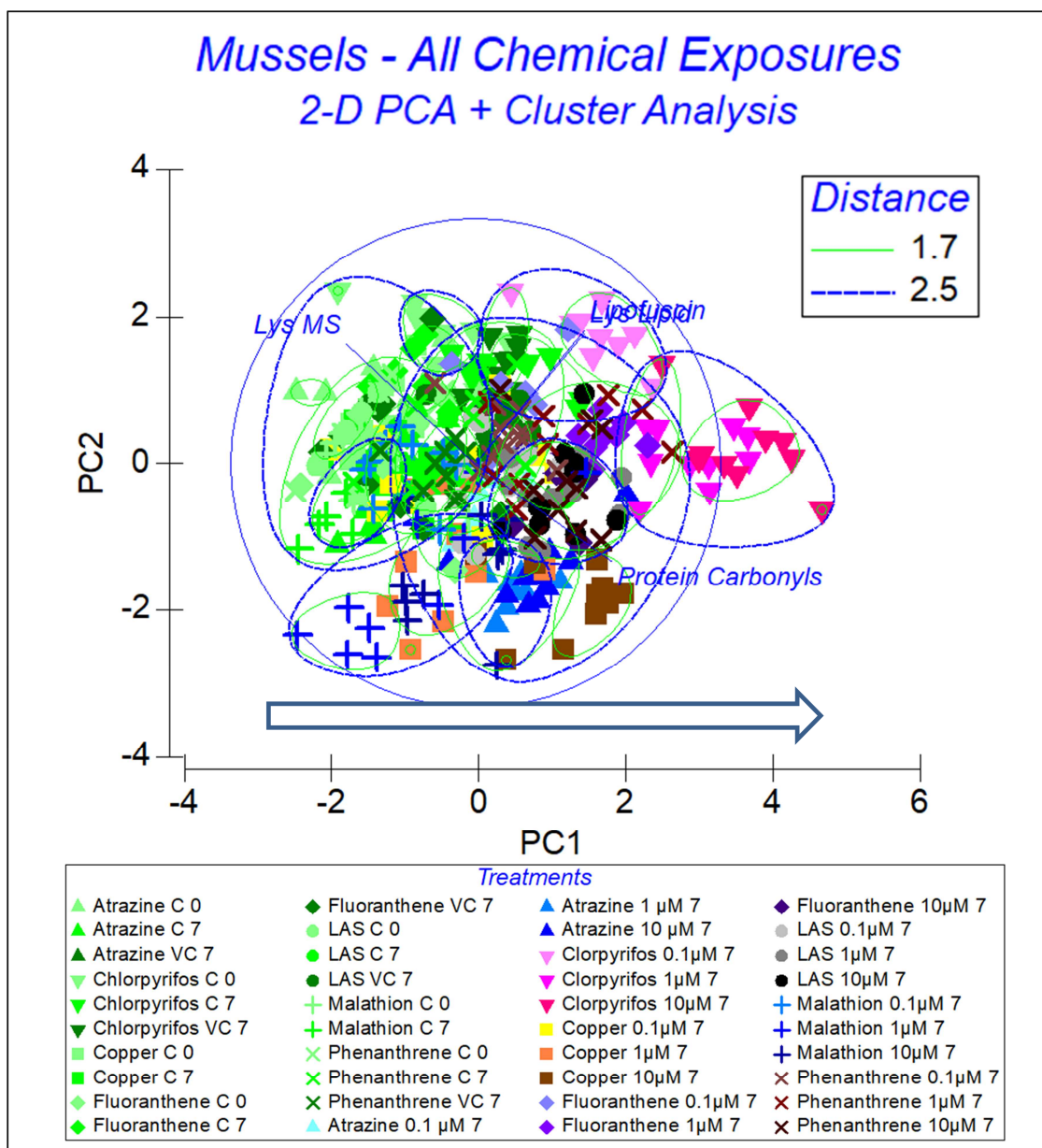


Fig. 6. Combined principal component and cluster analysis (i.e., elliptoid boundaries based on Euclidean distance) for all of the test compounds, based on the data for the four biomarkers in mussels. Vectors for the individual biomarkers are shown; and the large arrow indicates increasing cellular pathology. PC1 and PC2 captured 44.5% and 24.3% of the variation respectively.

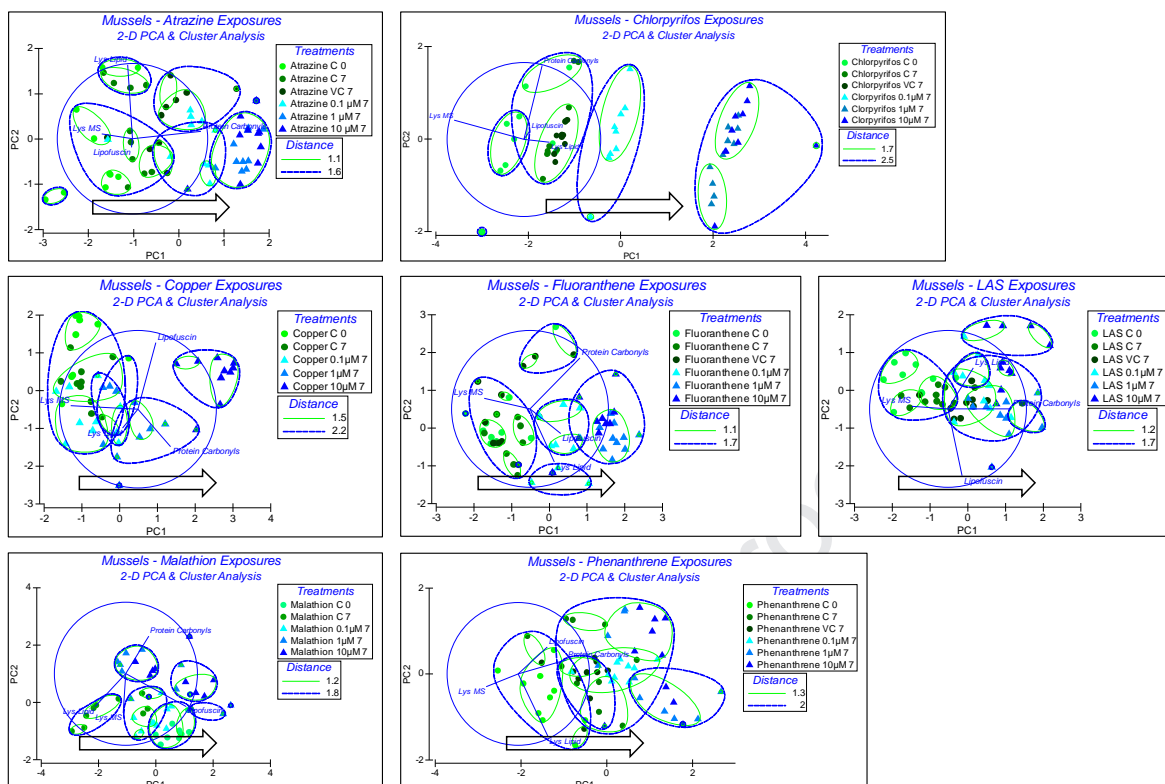


Fig. 7. Individual principal component and cluster analysis (i.e., ellipsoid boundaries based on Euclidean distance) for each of the test compounds, based on the data for the four biomarkers in mussels. Vectors for the individual biomarkers are shown; and the large arrow indicates increasing cellular pathology.

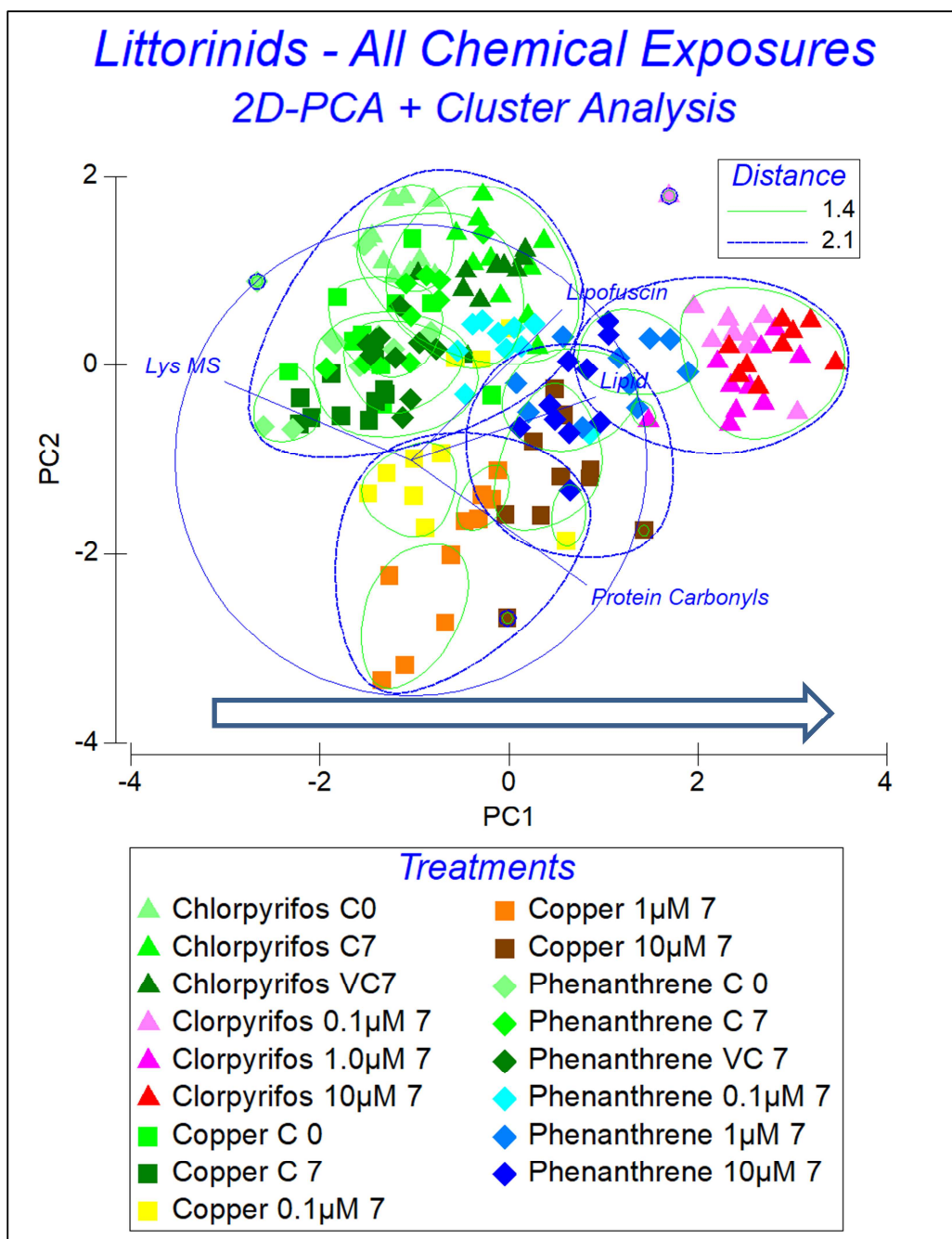


Fig. 8. Combined principal component and cluster analysis (i.e., ellipsoid boundaries based on Euclidean distance) for all of the test compounds, based on the data for the four biomarkers in periwinkles. Vectors for the individual biomarkers are shown; and the large arrow indicates increasing cellular pathology. PC1 and PC2 captured 54.8% and 22.4% of the variation respectively.

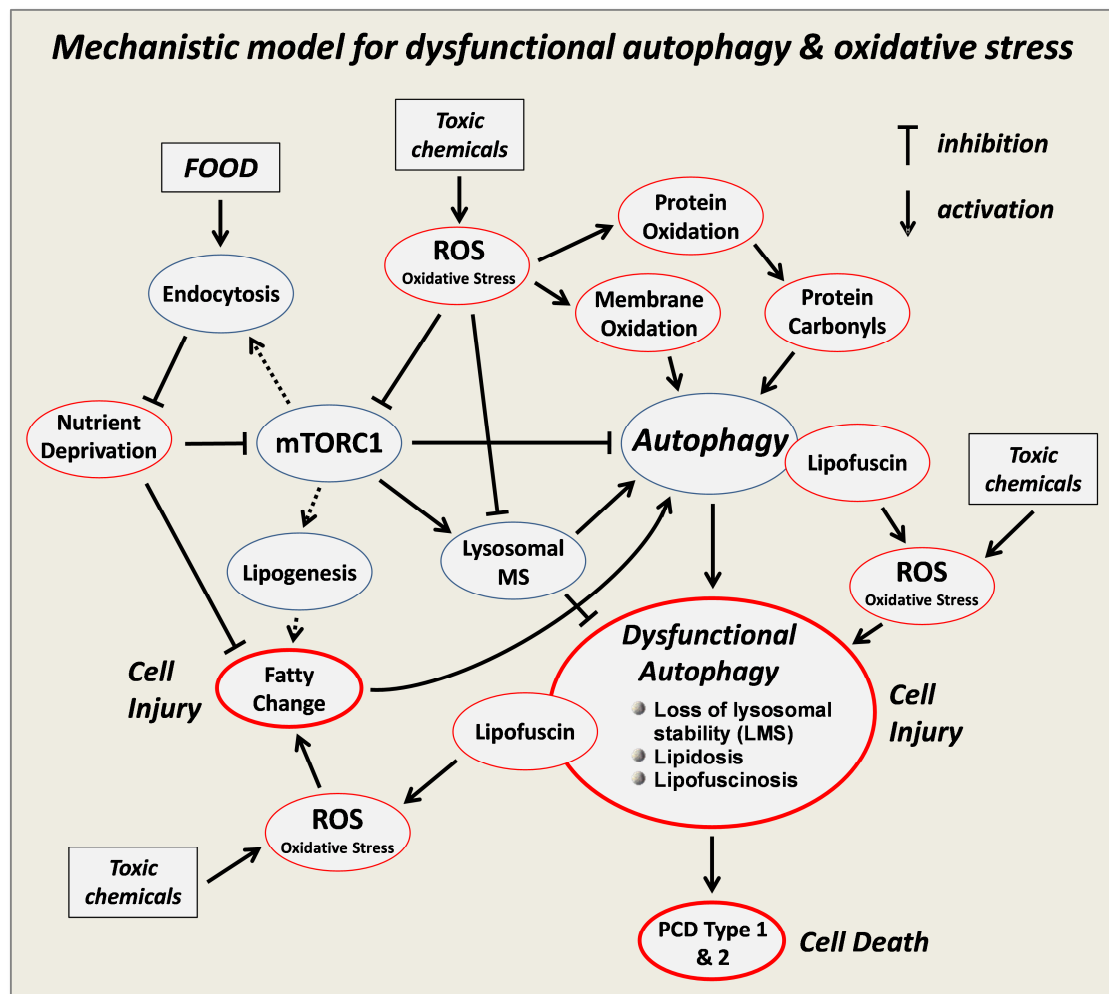


Fig. 9. Conceptual mechanistic model for the role of oxidative stress in dysregulation of autophagy and heterophagy (endocytosis of food) in hepatopancreatic digestive cells. Processes outlined in narrow red are considered to be potentially adverse; and those outlined in heavy red constitute cell injury and programmed cell death (PCD). mTORC1 is the mechanistic target for rapamycin complex 1 – a key component of the cellular signalling system. ROS – reactive oxygen species; dotted arrows indicate a generic process, although not yet confirmed in molluscs.

Highlights:

Failure of normal and physiologically augmented autophagic function as a pathological reaction to chemically induced stress appears to be a widespread phenomenon in many eukaryotic species, including molluscs, annelids and mammals, perhaps indicating that this type of reaction is generic. Evidence for the generic nature of this pathological reaction is supported by the observations from the present investigation and builds on previous studies. Dysfunctional autophagy is characteristic of a number of animal and human diseases, including neurodegenerative diseases, fibromyalgia, ocular pathologies, cardiovascular disease and obesity related conditions. Some of these disease conditions have been linked to uptake of harmful nanoscale materials derived from road traffic.

There are no conflicts of interest.

Journal Pre-proof